A Highly Selective Indole-based Sensor for Zn^{2+}, Cu^{2+} and Al^{3+} Ions with Multifunctional Applications

Gujuluva Gangatharan Vinoth Kumar, [a,*] Parkhi Sharma,[a] Govindhan Thiruppathi,[b] Palanisamy Sundararaj,[b] Apparao Draksharapu[a,*]

[a]*Southern Laboratories-208A, Department of Chemistry, Indian Institute of Technology Kanpur, Kanpur-208016, India. E-mail: appud@iitk.ac.in; ggvinoth1991@gmail.com*

[b]*Department of Zoology, Bharathiar University, Coimbatore, Tamil Nadu 641046, India.*

Water tolerance effect of R and R+Zn^{2+} systems

An ideal sensor should demonstrate robust performance in an aqueous phase. To evaluate the effect of water content on the receptor **R** and the **R**+Zn^{2+} complex, fluorescence experiments were conducted by progressively increasing the water percentage in an acetonitrile medium. As shown in Fig. S28, the fluorescence spectrum of **R** (10 µM) exhibited minimal changes with increasing water content in the pure acetonitrile medium, indicating good solubility and stability. In the case of **R**+Zn^{2+} system, the emission response at 497 nm remained stable up to 30% water content, confirming effective complexation. However, beyond 30% water content, a significant decrease in emission intensity was observed, attributed to aggregation-induced quenching and metal ion hydrolysis in highly aqueous environments. Based on these findings, the CH_3CN/H_2O (7:3, v/v) medium was selected as the optimal solvent system for all sensing investigations, as it provides a good balance of solubility, stability, and strong receptor-metal ion interactions.

Water sample analysis

The analytical applicability of receptor **R** was evaluated by detecting trace levels of Cu^{2+} and Al^{3+} ions in tap and drinking water samples. The water samples were initially filtered using Whatman filter paper and tested with **R**, where no changes were observed. Upon the addition of known quantities of Cu^{2+} and Al^{3+} ions to the filtered water samples, receptor **R** successfully detected the presence of these ions in each sample. A summary of the results is presented in Table S10.

Supporting Images and Tables

Table S1: Crystal data and structure refinement of **R**.

CCDC	**2414593**
Chemical formula	$C_{16}H_{14}N_2O_2$
Formula weight	266.29
Temperature	100
Wavelength	0.71073
Crystal size	0.12 × 0.11 × 0.1
Crystal system	Triclinic
Space group	P-1
α (Å)	78.9550(10)
β (Å)	78.4510(10)
γ (Å)	76.2820(10)
A	7.6488(3)
B	8.2023(3)
C	10.7408(4)
Volume	633.98(4)
Z	2
Density (calculated)	1.395
Absorption coefficient	0.094
F(000)	280.0
Goodness-of-fit on F^2	1.124
Final R indices I>2σ(I)	R_1 = 0.0399, wR_2 = 0.0962
R indices (all data)	R_1 = 0.0485, wR_2 = 0.1012

Table S2: Specific Bond lengths (Å) and bond angles (°) in the single crystal of **R**.

Bond distance (Å)	**R**	Bond Angles (°)	**R**
O2-C15	1.3636(15)	C10-N2-C9	124.97(10)
N2-C10	1.2992(15)	N1-C1-C2	130.09(11)
N2-C9	1.4593(14)	C8-N1-C1	108.75(10)
N1-C1	1.3780(15)	C2-C1-C6	122.41(11)
N1-C8	1.3748(16)	C4-C5-C6	118.23(10)
C5-C4	1.3845(16)	C15-C14-C13	120.84(11)
C5-C6	1.4076(16)	C4-C5-C9	123.28(10)
C5-C9	1.5128(16)	C5-C4-C3	121.42(11)
C11-C16	1.4244(16)	C6-C5-C9	118.49(10)
C11-C10	1.4219(16)	N2-C10-C11	123.26(11)
C11-C12	1.4219(16)	C10-C11-C16	120.23(10)
C15-C16	1.4346(16)	C5-C6-C1	119.32(11)
C15-C14	1.3717(17)	C10-C11-C12	119.05(11)
C16-O1	1.2978(14)	C5-C6-C7	133.74(11)
C1-C6	1.4147(16)	C12-C11-C16	120.73(10)
C1-C2	1.3999(17)	C1-C6-C7	106.93(10)
C14-C13	1.4134(18)	O2-C15-C16	118.33(10)
C4-C3	1.4086(17)	C8-C7-C6	106.64(11)
C6-C7	1.4343(16)	O2-C15-C14	120.46(11)
C7-C8	1.3655(17)	C13-C12-C11	120.25(11)
C12-C13	1.3682(17)	C14-C15-C16	121.20(11)
C2-C3	1.3816(17)	C7-C8-N1	110.18(11)

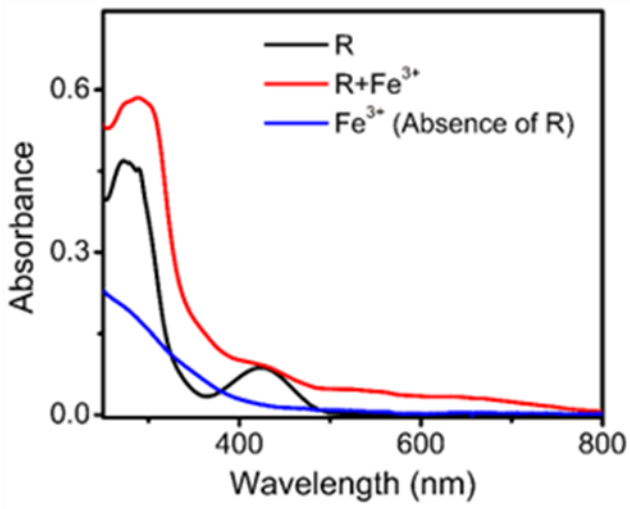

Fig. S1 UV-Vis absorption spectra of 80 µM of Fe^{3+} in the presence and absence of **R** in CH_3CN/H_2O (7:3, v/v) medium at room temperature.

Table S3: Comparison of the present sensor with the previously reported chemosensors.

Designed receptor	Selectivity	Method	Solvent system	Binding Constant (M^{-1}/M^{-2})	LOD (µM)	Application	Refs
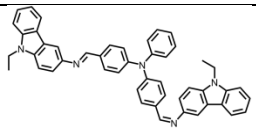	Al^{3+}	UV-Vis	EtOH	ND	0.67	Bio-imaging	[1]
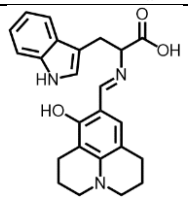	Al^{3+}	Fluorescence	Buffer solution	$1.13*10^3$	6.4	Bio-imaging	[2]
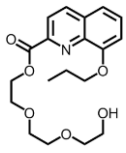	Al^{3+}	UV-Vis	CH_3CN/H_2O (95:5, v/v)	$4.6*10^4$	0.8	Water samples	[3]
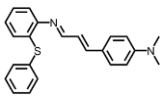	Cu^{2+}	UV-Vis	CH_3CN/H_2O (2:1, v/v)	$2.4*10^{10}$	2.85	Water samples	[4]
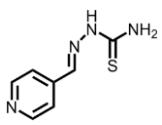	Cu^{2+}	UV-Vis	$MeOH/H_2O$ (1:1, v/v)	$2.4*10^2$	1.7	Water samples	[5]

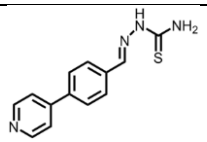	Cu^{2+}	UV-Vis	$MeOH/H_2O$ (1:1, v/v)	$2.69*10^4$	10.67	Water samples, and Paper strip	[6]
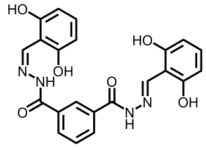	Al^{3+}	Fluorescence	CH_3CN	$11*10^5$	0.44	Nil	[7]
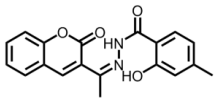	Al^{3+}	Fluorescence	DMF/H_2O (9:1, v/v)	$3.21*10^6$	6.7	Nil	[8]
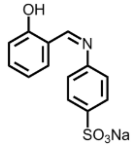	Al^{3+}	Fluorescence	HEPES buffer	$5.69*10^3$	1.67	Bio-imaging, and Paper strip	[9]
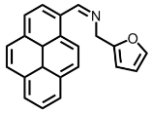	Al^{3+}	Fluorescence	DMF/H_2O (9:1, v/v)	$1.1*10^3$	1.04	Paper strip	[10]
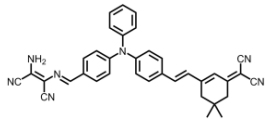	Cu^{2+}	Fluorescence	CH_3CN	$1.18*10^4$	1.56	Nil	[11a]
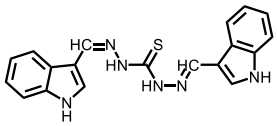	Cu^{2+}	Fluorescence	CH_3CN-H_2O (1:2, v/v)	$2.63*10^{10}$	0.0893	Bio-imaging	[11b]
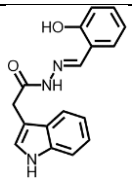	Zn^{2+}	Fluorescence	DMSO-Tris buffer	$1.6*10^4$	0.41	Bio-imaging, and Water samples	12
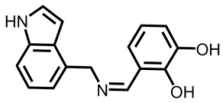	Al^{3+}	UV-Vis	CH_3CN / H_2O (7:3, v/v)	$2.18*10^4$	**0.45**	Bio-imaging, Logic circuits, Security keypad lock, and Water samples	Present Work
	Cu^{2+}	UV-Vis		$1.86*10^4$	**0.57**		
	Zn^{2+}	Fluorescence		$7.15*10^4$	**0.056**		

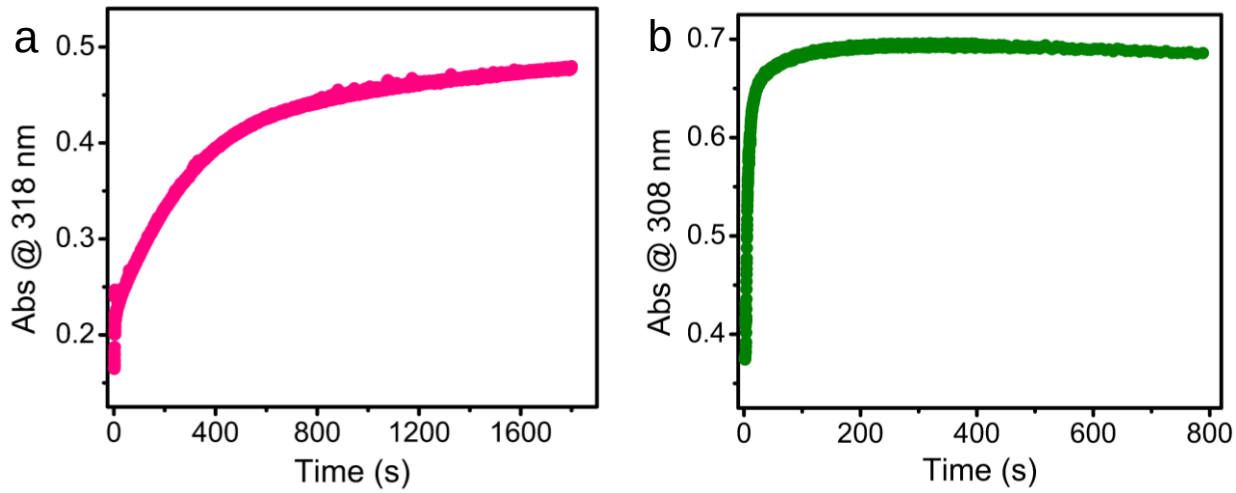

Fig. S2 UV-Vis time response of (a) **R**-Cu^{2+}, and (b) **R**-Al^{3+} complex system in CH_3CN/H_2O (7:3, v/v) medium at room temperature.

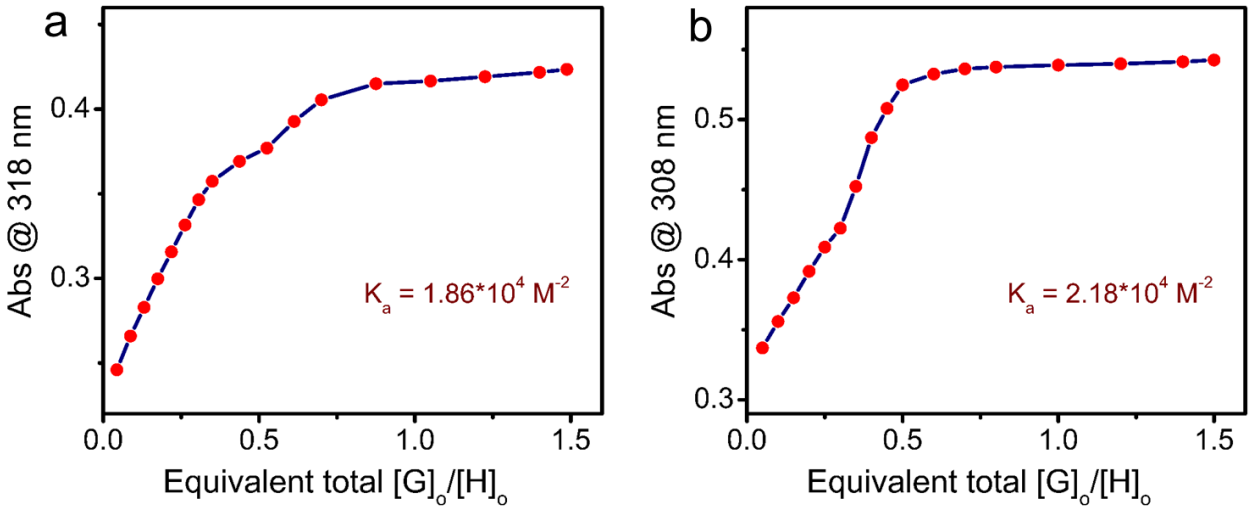

Fig. S3 (a) BindFit plot of **R**-Cu^{2+} complex (at λ_{abs} = 318 nm), and (b) BindFit plot of **R**-Al^{3+} complex (at λ_{abs} = 308 nm).

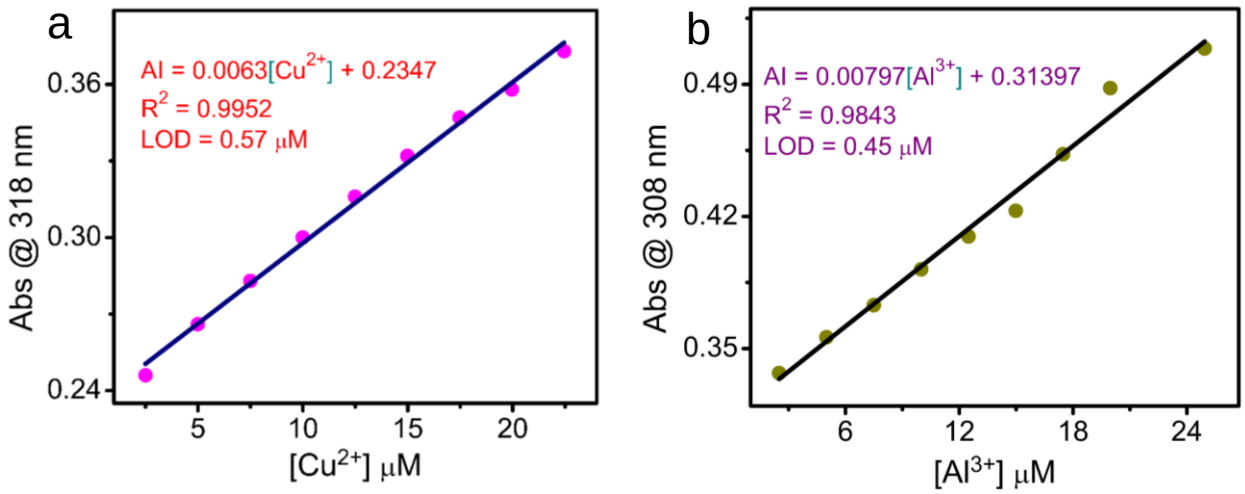

Fig. S4 UV-Vis absorption spectroscopic calibration curve of (a) **R**-Cu^{2+}, and (b) **R**-Al^{3+}.

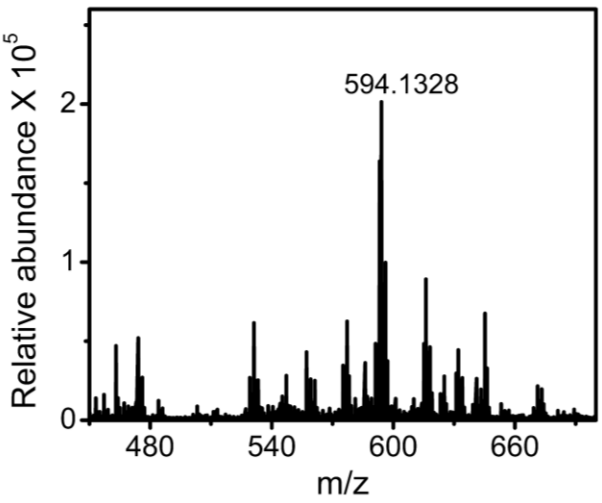

Fig. S5 Positive-ion ESI mass spectrum of **R**+Cu^{2+}.

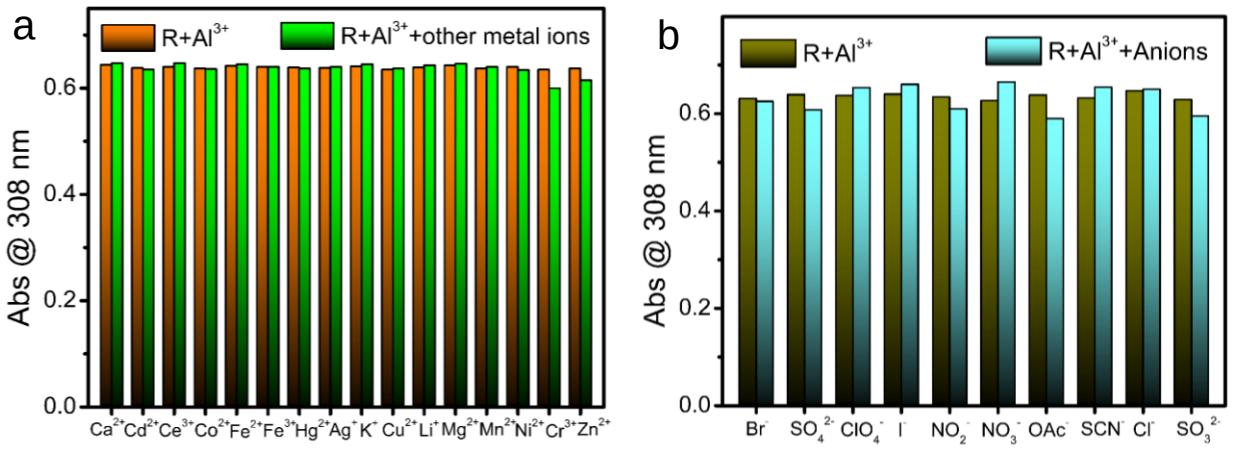

Fig. S6 (a & b) Interference studies of **R** with 1 eq. of Al^{3+} and 3 eq. of other metal ions and anions in CH_3CN/H_2O (7:3, v/v) medium at room temperature.

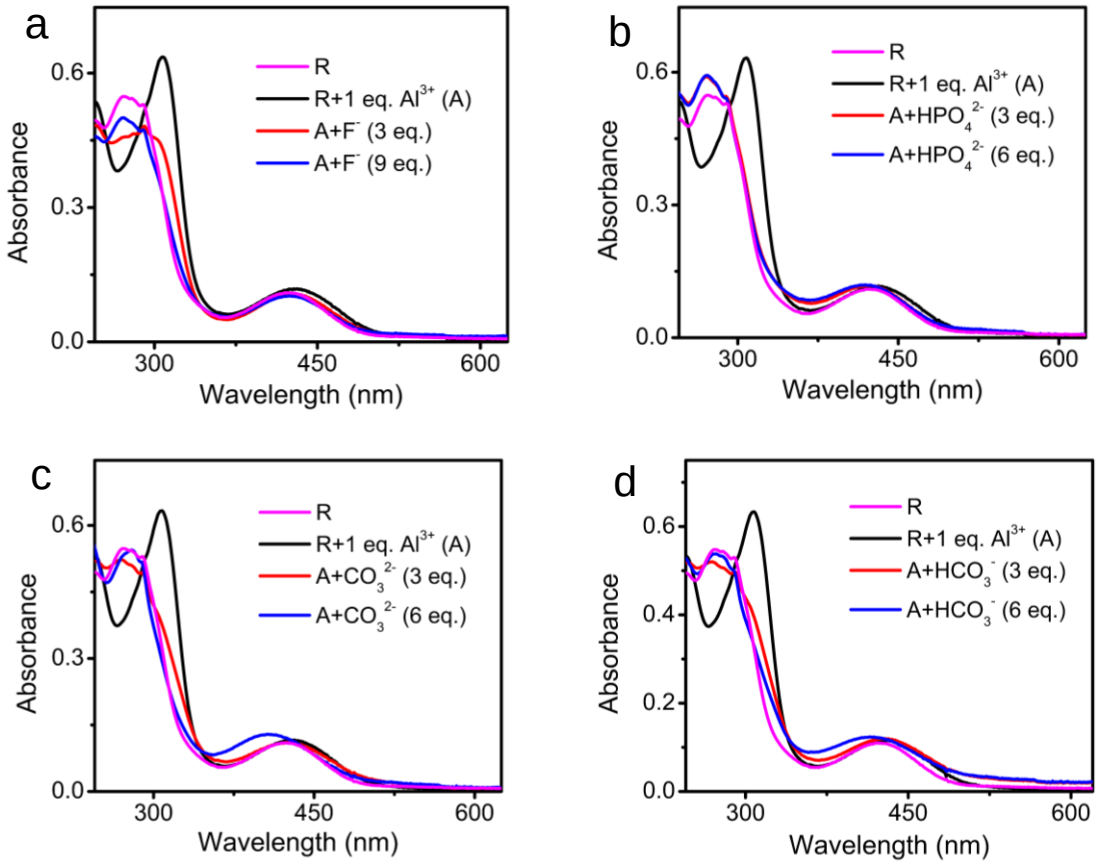

Fig. S7 UV-Vis absorption spectra of **R**+Al^{3+} with interfering anions (a) F^-, (b) HPO_4^{2-}, (c) CO_3^{2-}, and (d) HCO_3^- in CH_3CN/H_2O (7:3, v/v) medium at room temperature.

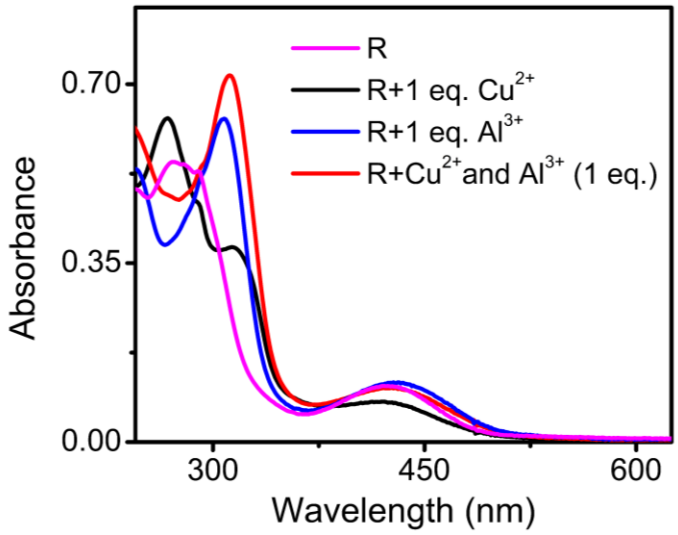

Fig. S8 Absorption spectra of **R**, **R**+Cu^{2+}, **R**+Al^{3+}, and **R**+Cu^{2+}+Al^{3+} in a mixture of 7:3 CH_3CN/H_2O at room temperature. [**R**] = [Cu^{2+}] = [Al^{3+}] = 40 μM.

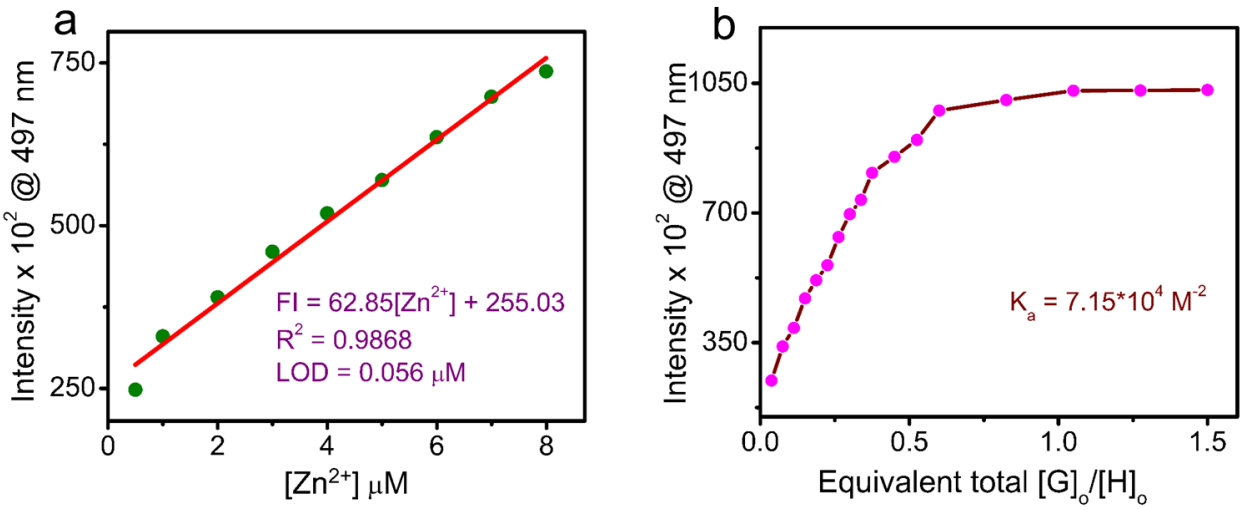

Fig. S9 (a) Calibration curve of **R**-Zn^{2+} system, (b) BindFit plot of **R**-Zn^{2+} complex ($\lambda_{emission}$ = 497 nm).

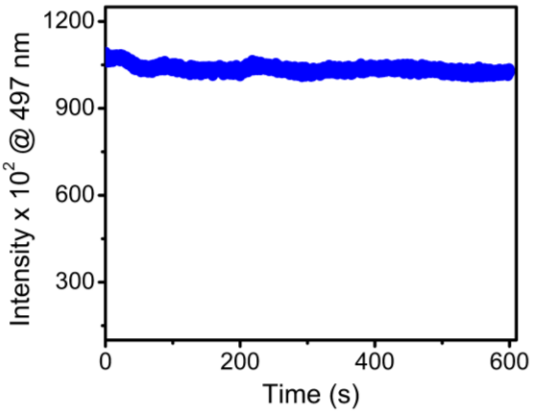

Fig. S10 Fluorescence time response of **R**+Zn^{2+} complex system.

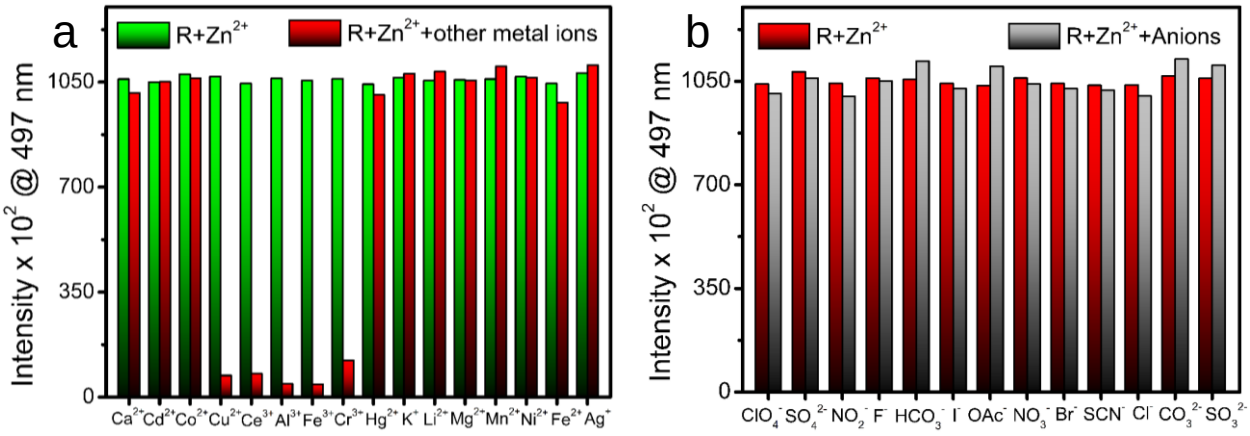

Fig. S11 Competitive study of **R**+Zn^{2+} complex over 3 eq. of various metal ions (a) and anions (b) in CH_3CN/H_2O (7:3, v/v) medium at room temperature.

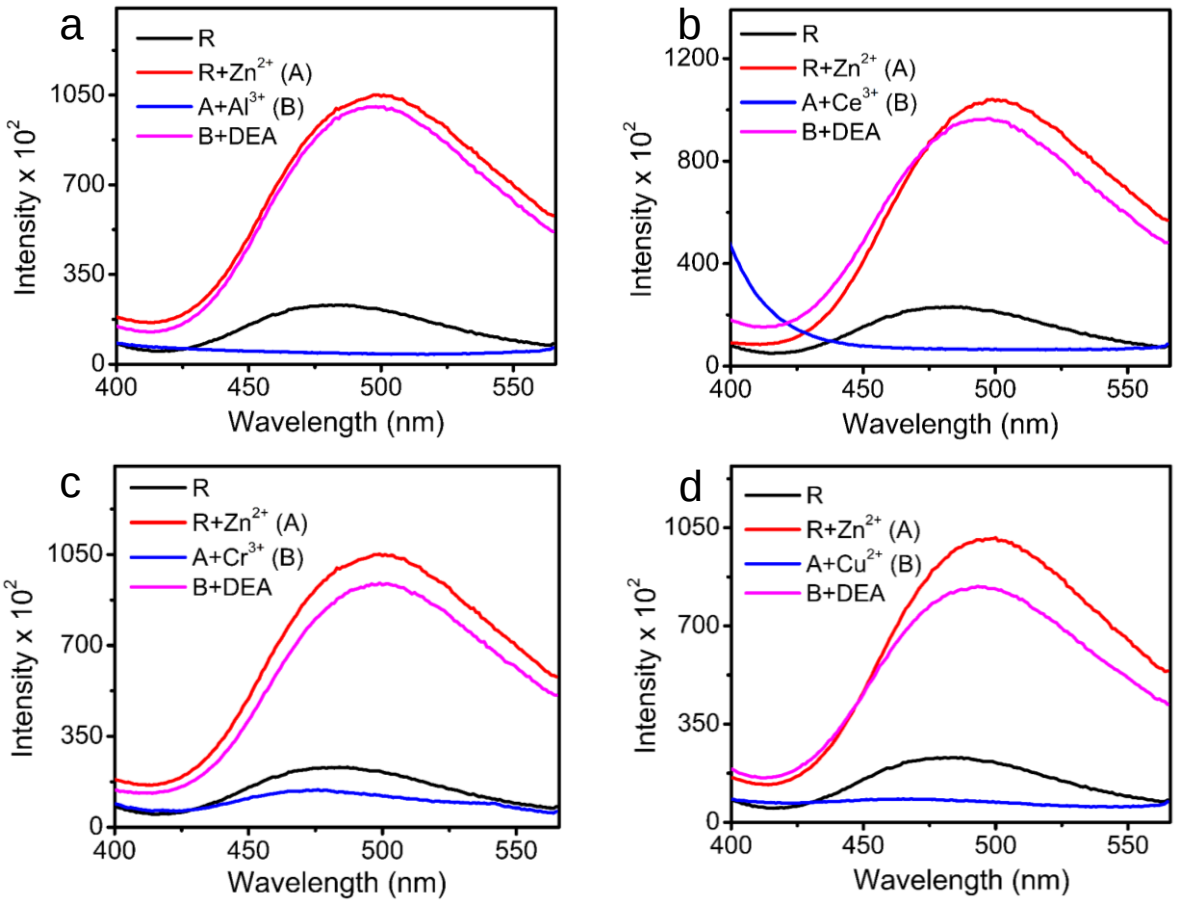

Fig. S12 Fluorescence spectra of **R**+Zn^{2+} with interfering metal ions and DEA in 7:3 CH_3CN/H_2O.

[**R**] = [Zn^{2+}] = 10 μM, [Al^{3+}, Ce^{3+}, Cr^{3+}, Cu^{2+}] = 3 eq. [DEA] = 5 eq.

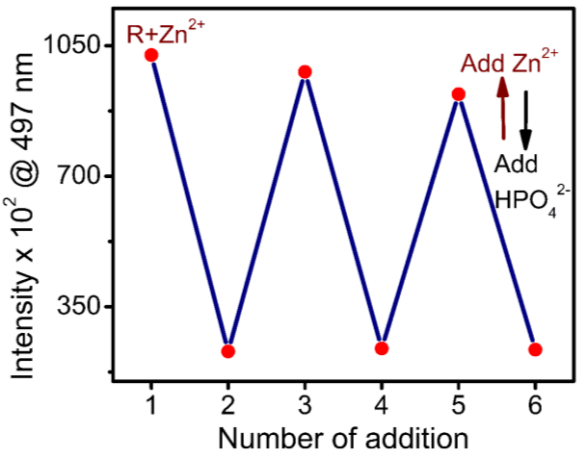

Fig. S13 Durability studies of **R** by the alternate treatment of Zn^{2+} and HPO_4^{2-}.

Table S4. Fluorescence lifetime measurements of receptor **R**, **R**+Zn^{2+}, and **R**+Zn^{2+}+HPO_4^{2-}.

Compound	τ_1	τ_2	τ_3	α_1	α_2	α_3	χ^2	τ_{av} (ns)
R	53.6294	1.2257	383.0135	0.0070	1.3486	0.0021	1.4920	2.086
R+Zn^{2+}	39.0484	290.7679	1.0884	0.0183	0.0122	1.5322	1.3898	3.794
R+Zn^{2+}+HPO_4^{2-}	40.5635	335.1841	0.7793	0.0124	0.0037	2.6169	1.3153	1.437

τ_{av} represents the average lifetime. τ_1, τ_2 denotes the exponential fitting lifetime values. While α_1, α_2 indicates their respective contributions to the average lifetime.

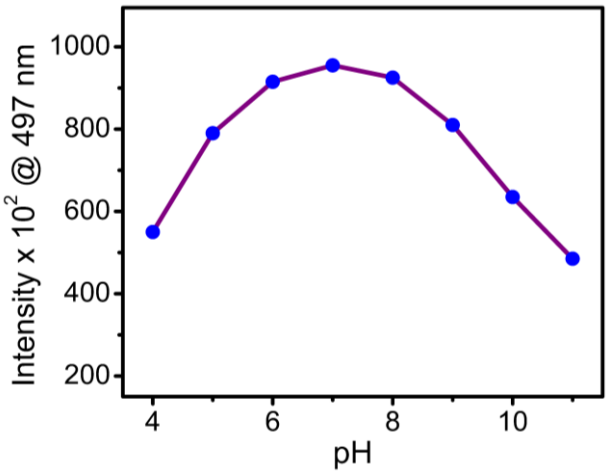

Fig. S14. The effect of pH on **R**+Zn^{2+} system.

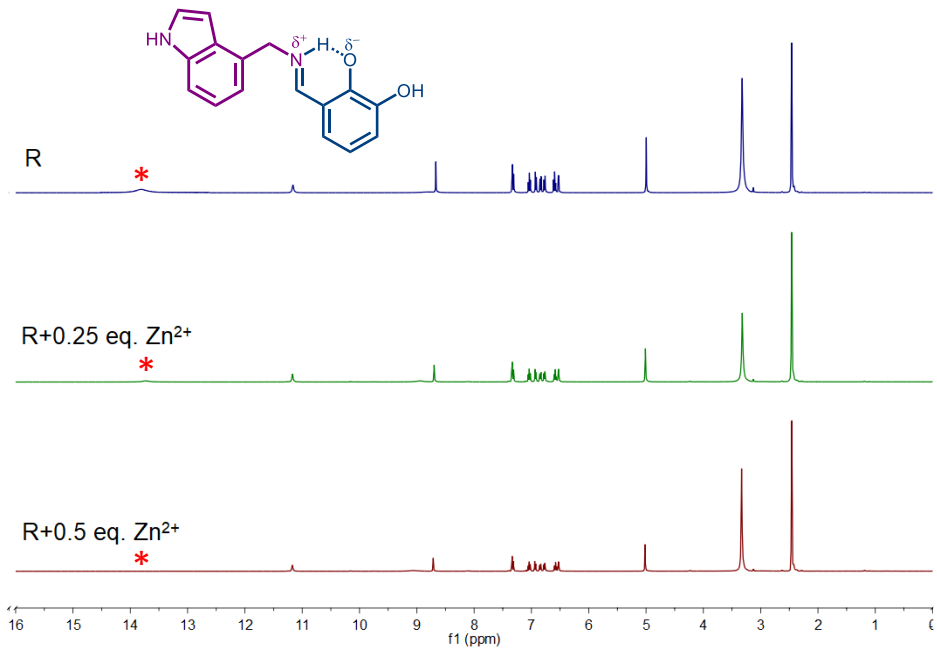

Fig. S15 ^{1}H NMR (400 MHz) titration of **R** with different concentrations of Zn^{2+} in DMSO-d_6 at room temperature.

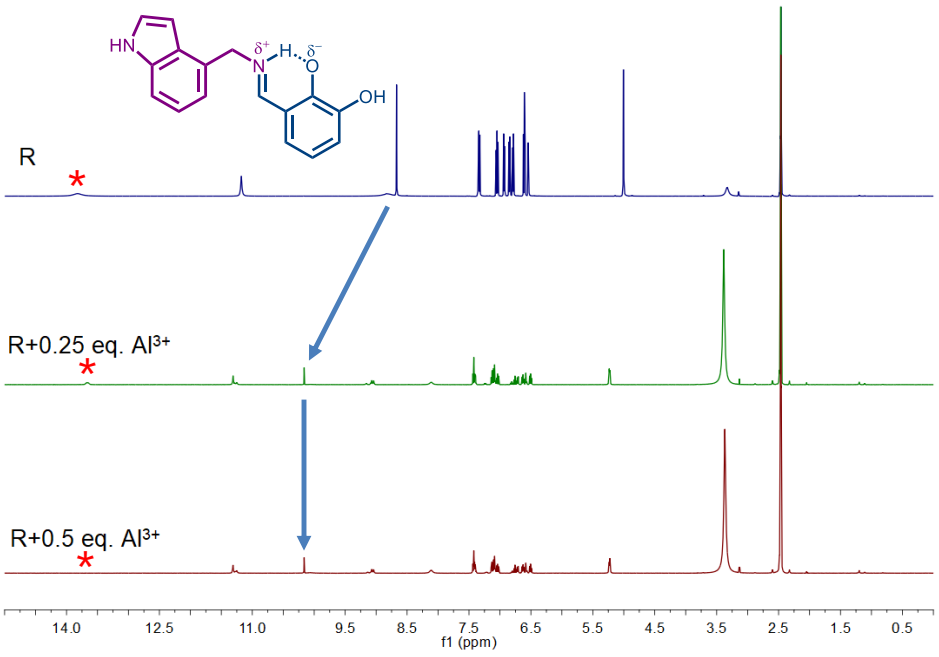

Fig. S16 ^{1}H NMR (500 MHz) titration of **R** with different concentrations of Al^{3+} in DMSO-d_6 at room temperature.

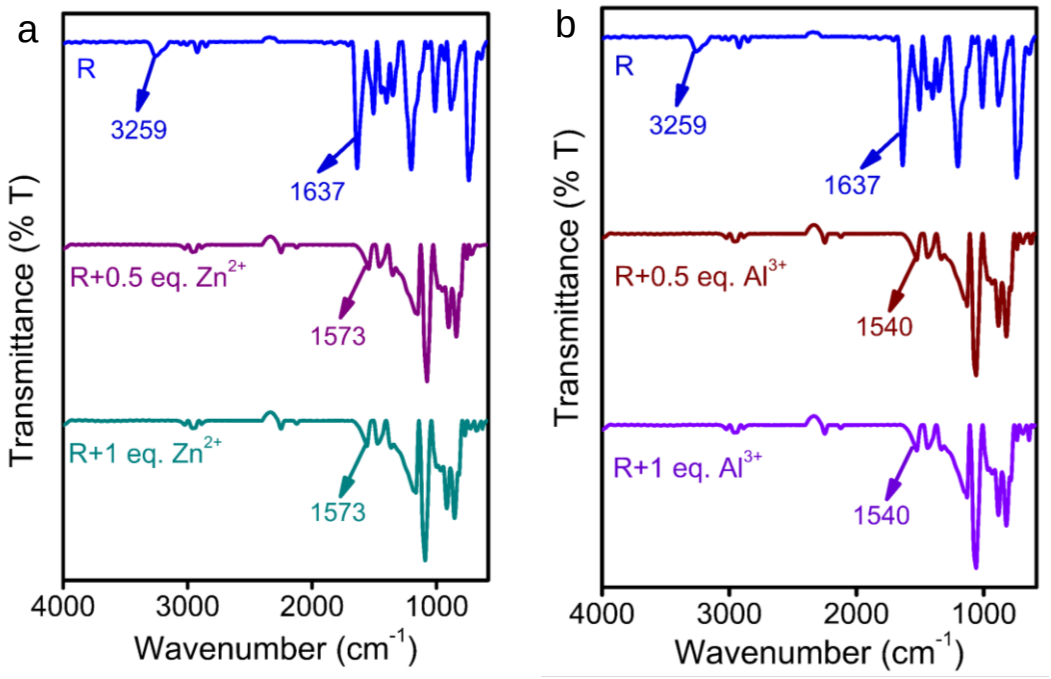

Fig. S17 IR titration of **R** with different concentrations of Zn^{2+}, and Al^{3+}.

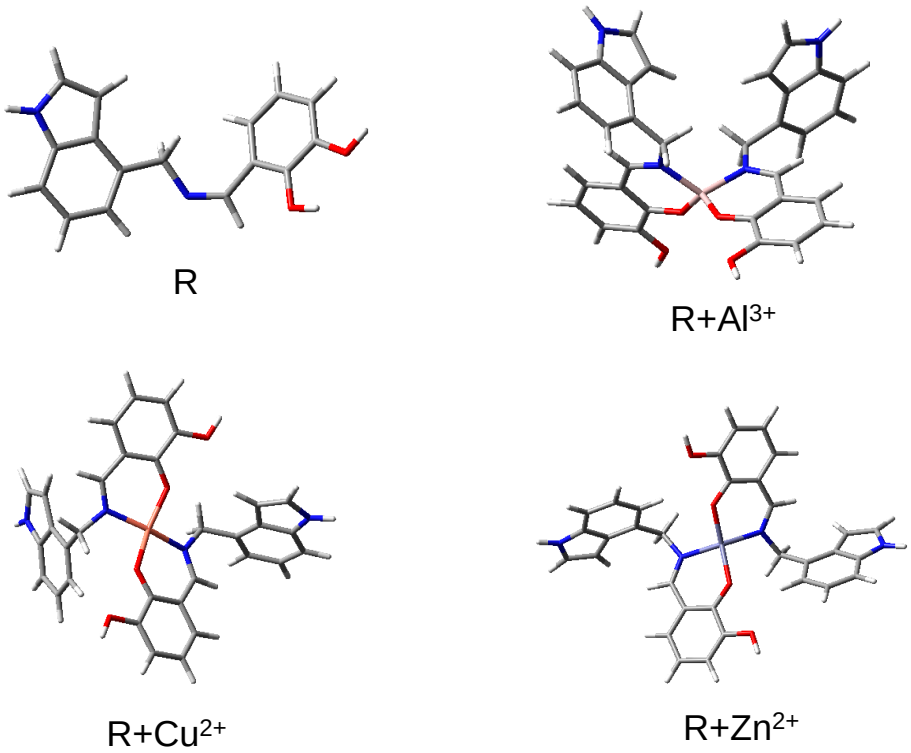

Fig. S18 Ground state optimized geometry of **R**, **R**+Cu^{2+}, **R**+Al^{3+}, and **R**+Zn^{2+} complexes by using the DFT/B3LYP method.

Table S5. Computational results of the optimized structure of **R**.

1	6	0	-0.639369	-0.235352	-0.844358
2	7	0	0.174225	-1.424796	-1.027954
3	7	0	-4.859438	1.382423	0.686016
4	6	0	-3.993798	2.423812	0.418794
5	6	0	-2.796478	1.920801	-0.012847
6	6	0	-2.914611	0.487304	-0.017359
7	6	0	-2.037356	-0.565522	-0.355747
8	6	0	-2.503547	-1.865825	-0.235824
9	6	0	-3.810417	-2.143212	0.210808
10	6	0	-4.691983	-1.129528	0.548982
11	6	0	-4.227070	0.183082	0.428484
12	6	0	1.435631	-1.420658	-0.865316
13	6	0	2.369584	-0.308021	-0.549897
14	6	0	3.470178	-0.588106	0.271551
15	6	0	4.416214	0.409373	0.552101
16	6	0	4.284699	1.679086	0.012120
17	6	0	3.201866	1.962345	-0.823502
18	6	0	2.258866	0.982045	-1.097314
19	8	0	3.619213	-1.830128	0.805589
20	8	0	5.442410	0.010210	1.378534
21	1	0	-0.733187	0.270846	-1.816560

22	1	0	-0.181146	0.492798	-0.160508
23	1	0	-5.803292	1.482819	1.017664
24	1	0	-4.306158	3.446664	0.560006
25	1	0	-1.936617	2.509143	-0.291307
26	1	0	-1.835725	-2.676393	-0.495233
27	1	0	-4.130812	-3.176114	0.290706
28	1	0	-5.697582	-1.346454	0.892629
29	1	0	1.926296	-2.390957	-0.962579
30	1	0	5.024093	2.441903	0.237086
31	1	0	3.105207	2.948807	-1.260156
32	1	0	1.441736	1.201489	-1.770676
33	1	0	4.437534	-1.833995	1.319306
34	1	0	6.058697	0.735660	1.516152

Table S6. Computational results of the optimized structure of **R**+Cu^{2+}.

1	6	0	-3.234136	-0.032622	1.258623
2	7	0	-2.084119	0.904550	1.065207
3	7	0	-5.421898	0.471390	-3.045402
4	6	0	-5.310261	1.710723	-2.411017
5	6	0	-4.667957	1.546121	-1.196105
6	6	0	-4.359713	0.136222	-1.054102
7	6	0	-3.730395	-0.644432	-0.043984
8	6	0	-3.615317	-2.027227	-0.255902

9	6	0	-4.107481	-2.646696	-1.435291
10	6	0	-4.730712	-1.898969	-2.443607
11	6	0	-4.847271	-0.511726	-2.235018
12	6	0	-2.271078	2.174862	1.328703
13	6	0	-1.323038	3.260912	1.203734
14	6	0	0.009708	3.047582	0.722656
15	6	0	0.859694	4.201904	0.610994
16	6	0	0.411375	5.474082	0.962896
17	6	0	-0.911980	5.668262	1.440735
18	6	0	-1.761499	4.573627	1.556245
19	8	0	0.493423	1.858520	0.380373
20	6	0	1.924613	0.117555	-1.468075
21	7	0	1.211313	-0.743856	-0.449211
22	7	0	6.450014	0.590776	0.109975
23	6	0	5.549873	1.291970	0.925603
24	6	0	4.265943	1.140871	0.433535
25	6	0	4.360563	0.305090	-0.744142
26	6	0	3.396468	-0.188557	-1.663225
27	6	0	3.855674	-0.965189	-2.740242
28	6	0	5.234058	-1.269224	-2.911808
29	6	0	6.197469	-0.806424	-2.003717
30	6	0	5.743645	-0.019809	-0.926929

31	6	0	1.618100	-1.975662	-0.256095
32	6	0	1.019151	-2.986472	0.591436
33	6	0	-0.181054	-2.742465	1.335350
34	6	0	-0.735268	-3.847496	2.068817
35	6	0	-0.106400	-5.091222	2.098844
36	6	0	1.099149	-5.308859	1.380897
37	6	0	1.643526	-4.269644	0.633483
38	8	0	-0.801631	-1.569636	1.376946
39	29	0	-0.313678	0.102916	0.544750
40	8	0	2.155821	3.949883	0.138165
41	8	0	-1.941222	-3.586287	2.742338
42	1	0	-4.053811	0.514947	1.752951
43	1	0	-2.885619	-0.831181	1.917194
44	1	0	-5.847759	0.309488	-3.946369
45	1	0	-5.690246	2.610944	-2.872270
46	1	0	-4.439028	2.341864	-0.504136
47	1	0	-3.131894	-2.631432	0.506105
48	1	0	-3.995575	-3.721706	-1.555547
49	1	0	-5.108171	-2.375205	-3.345706
50	1	0	-3.262716	2.475732	1.691082
51	1	0	1.083221	6.327795	0.870723
52	1	0	-1.247394	6.665187	1.710774

53	1	0	-2.778762	4.706284	1.921130
54	1	0	1.780304	1.146742	-1.132669
55	1	0	1.382280	-0.008564	-2.415897
56	1	0	7.448956	0.540260	0.247466
57	1	0	5.897027	1.842812	1.788015
58	1	0	3.365887	1.591227	0.827412
59	1	0	3.138454	-1.341125	-3.468244
60	1	0	5.544377	-1.871861	-3.762225
61	1	0	7.250586	-1.044066	-2.136164
62	1	0	2.506590	-2.308270	-0.800617
63	1	0	-0.546432	-5.905248	2.675688
64	1	0	1.579258	-6.282351	1.414127
65	1	0	2.558947	-4.424144	0.065130
66	1	0	2.677908	4.774707	0.059903
67	1	0	-2.240725	-4.369788	3.248083

Table S7. Computational results of the optimized structure of **R**+Al^{3+}.

1	6	0	-1.612571	0.247297	1.656135
2	7	0	-1.596117	-0.592785	0.389250
3	7	0	-4.032643	4.266545	0.523531
4	6	0	-2.873123	4.163647	-0.242452
5	6	0	-2.206247	2.993998	0.088205
6	6	0	-2.983444	2.334235	1.114853

7	6	0	-2.822626	1.129955	1.855029
8	6	0	-3.804104	0.796580	2.802678
9	6	0	-4.932638	1.628434	3.032259
10	6	0	-5.109210	2.821002	2.317572
11	6	0	-4.128532	3.158581	1.365761
12	6	0	-2.695428	-0.718972	-0.342714
13	6	0	-2.864213	-1.528798	-1.527294
14	6	0	-1.802822	-2.330442	-2.056878
15	6	0	-2.036516	-3.110882	-3.220445
16	6	0	-3.299847	-3.090126	-3.828416
17	6	0	-4.352062	-2.300848	-3.303848
18	6	0	-4.140549	-1.526199	-2.167587
19	8	0	-0.587388	-2.340718	-1.465668
20	6	0	1.611567	0.247976	-1.655066
21	7	0	1.595026	-0.592798	-0.388629
22	7	0	4.037310	4.264091	-0.523522
23	6	0	2.878021	4.162639	0.243003
24	6	0	2.209441	2.993902	-0.087437
25	6	0	2.985333	2.333176	-1.114449
26	6	0	2.822603	1.129136	-1.854590
27	6	0	3.803158	0.794581	-2.802776
28	6	0	4.932613	1.625021	-3.032915

29	6	0	5.111100	2.817312	-2.318238
30	6	0	4.131334	3.156091	-1.365906
31	6	0	2.694228	-0.719458	0.343412
32	6	0	2.862739	-1.529913	1.527608
33	6	0	1.801234	-2.331866	2.056521
34	6	0	2.034712	-3.113003	3.219665
35	6	0	3.297914	-3.092592	3.827903
36	6	0	4.350230	-2.303001	3.304011
37	6	0	4.138947	-1.527699	2.168158
38	8	0	0.585923	-2.341824	1.465068
39	13	0	-0.000641	-1.576543	-0.000060
40	8	0	-0.963024	-3.856218	-3.690398
41	8	0	0.961134	-3.858629	3.688952
42	1	0	-0.696699	0.853682	1.629839
43	1	0	-1.510128	-0.458313	2.489139
44	1	0	-4.695098	5.028915	0.482058
45	1	0	-2.609547	4.925225	-0.961864
46	1	0	-1.277866	2.661605	-0.354039
47	1	0	-3.695822	-0.115230	3.386475
48	1	0	-5.665200	1.336524	3.779350
49	1	0	-5.970396	3.458187	2.501027
50	1	0	-3.572853	-0.159802	-0.016235

51	1	0	-3.475233	-3.691544	-4.719097
52	1	0	-5.319719	-2.306755	-3.794983
53	1	0	-4.941809	-0.916885	-1.756894
54	1	0	0.696549	0.855616	-1.627710
55	1	0	1.507472	-0.457070	-2.488335
56	1	0	4.700765	5.025606	-0.482329
57	1	0	2.615768	4.924515	0.962581
58	1	0	1.280819	2.662700	0.355201
59	1	0	3.693417	-0.117047	-3.386579
60	1	0	5.664399	1.332233	-3.780422
61	1	0	5.972970	3.453436	-2.502165
62	1	0	3.571749	-0.160228	0.017320
63	1	0	3.473126	-3.694523	4.718273
64	1	0	5.317785	-2.309192	3.795346
65	1	0	4.940292	-0.918166	1.757960
66	1	0	-1.197341	-4.405186	-4.467252
67	1	0	1.195299	-4.408093	4.465501

Table S8. Computational results of the optimized structure of **R**+Zn^{2+}.

1	6	0	-2.707014	0.476498	-1.421495
2	7	0	-1.821612	-0.576463	-0.806929
3	7	0	-7.445747	0.047162	-0.545709
4	6	0	-7.095077	-0.649080	-1.704865

5	6	0	-5.736959	-0.503766	-1.932307
6	6	0	-5.204917	0.325791	-0.866806
7	6	0	-3.910302	0.823816	-0.556201
8	6	0	-3.759868	1.633648	0.581831
9	6	0	-4.868238	1.941699	1.414183
10	6	0	-6.155528	1.459029	1.134200
11	6	0	-6.305500	0.655440	-0.011338
12	6	0	-2.305904	-1.794431	-0.690589
13	6	0	-1.677111	-2.951444	-0.082997
14	6	0	-0.376243	-2.910844	0.535889
15	6	0	0.114597	-4.140052	1.102266
16	6	0	-0.632756	-5.315754	1.061522
17	6	0	-1.916524	-5.337790	0.454397
18	6	0	-2.423001	-4.171782	-0.105943
19	8	0	0.379883	-1.821700	0.596723
20	8	0	1.389626	-4.072328	1.684905
21	6	0	2.707137	-0.476525	-1.421396
22	7	0	1.821668	0.576354	-0.806784
23	7	0	7.445859	-0.046732	-0.545800
24	6	0	7.095081	0.649436	-1.704967
25	6	0	5.736961	0.504012	-1.932335
26	6	0	5.205044	-0.325591	-0.866808

27	6	0	3.910490	-0.823743	-0.556149
28	6	0	3.760182	-1.633576	0.581898
29	6	0	4.868617	-1.941519	1.414203
30	6	0	6.155849	-1.458725	1.134164
31	6	0	6.305695	-0.655128	-0.011384
32	6	0	2.305916	1.794330	-0.690332
33	6	0	1.677041	2.951292	-0.082726
34	6	0	0.376194	2.910584	0.536200
35	6	0	-0.114880	4.139831	1.102287
36	6	0	0.632310	5.315631	1.061390
37	6	0	1.916174	5.337711	0.454467
38	6	0	2.422834	4.171689	-0.105678
39	8	0	-0.379920	1.821427	0.596880
40	30	0	0.000011	-0.000104	-0.021519
41	8	0	-1.389984	4.072051	1.684754
42	1	0	-3.032368	0.135693	-2.414143
43	1	0	-2.083142	1.364397	-1.555679
44	1	0	-8.374662	0.103445	-0.153885
45	1	0	-7.835332	-1.189451	-2.277260
46	1	0	-5.196270	-0.925490	-2.767987
47	1	0	-2.777844	2.028468	0.834776
48	1	0	-4.708053	2.566785	2.289206

49	1	0	-6.998691	1.700187	1.777723
50	1	0	-3.315499	-1.982838	-1.075170
51	1	0	-0.227931	-6.227805	1.501210
52	1	0	-2.489086	-6.260317	0.434566
53	1	0	-3.407579	-4.172135	-0.570721
54	1	0	1.661729	-4.943047	2.041553
55	1	0	3.032443	-0.135659	-2.414038
56	1	0	2.083340	-1.364475	-1.555597
57	1	0	8.374792	-0.102905	-0.154003
58	1	0	7.835263	1.189859	-2.277407
59	1	0	5.196197	0.925677	-2.767996
60	1	0	2.778206	-2.028478	0.834897
61	1	0	4.708527	-2.566612	2.289237
62	1	0	6.999062	-1.699798	1.777653
63	1	0	3.315526	1.982793	-1.074845
64	1	0	0.227303	6.227715	1.500844
65	1	0	2.488681	6.260273	0.434672
66	1	0	3.407506	4.172064	-0.570256
67	1	0	-1.662254	4.942804	2.041192

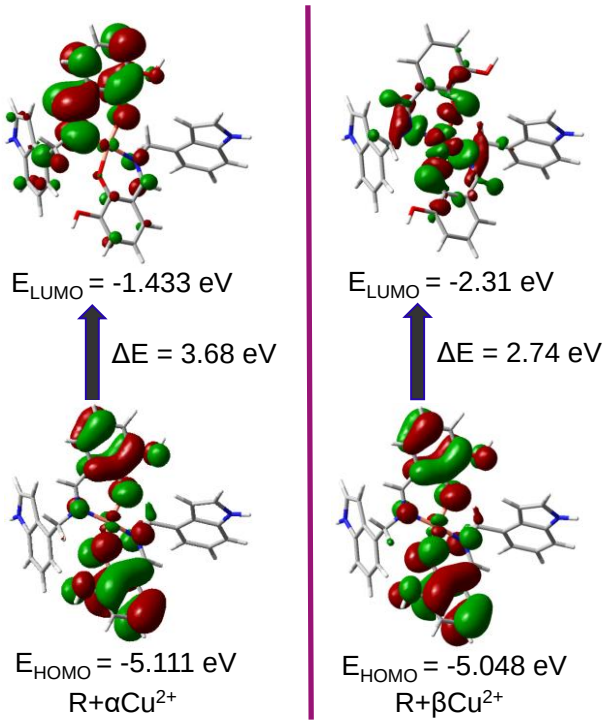

Fig. S19 Frontier molecular orbital structures of **R**+Cu^{2+} complex.

Table S9. Molecular docking scores of **R** and metal complexes with DNA and BSA.

Compound	Binding free energy ($\Delta G_{binding}$)$^{\alpha}$	Vdw_hb_desolv energy ($\Delta G_{vdW+hb+desolv}$)	Electrostatic energy (ΔG_{elec})	Total internal energy (ΔG_{total})	Torsional free energy (ΔG_{tor})	Unbound system energy (ΔG_{unb})
DNA						
R	-6.36	-7.69	-0.16	-1.27	1.49	-1.27
R+Al^{3+}	-7.11	-8.63	-0.27	-3.67	1.79	-3.67
R+Cu^{2+}	-6.68	-8.47	-0.29	-3.30	1.79	-3.30
R+Zn^{2+}	-6.35	-7.92	-0.22	-3.31	1.79	-3.31
BSA						
R	-5.49	-6.61	-0.37	-2.03	1.49	-0.23
R+Al^{3+}	-5.25	-7.13	-0.1	-4.75	1.79	-4.75
R+Cu^{2+}	-4.34	-5.99	-0.13	-4.90	1.79	-4.90
R+Zn^{2+}	-4.73	-6.61	0.08	-4.82	1.79	-4.82

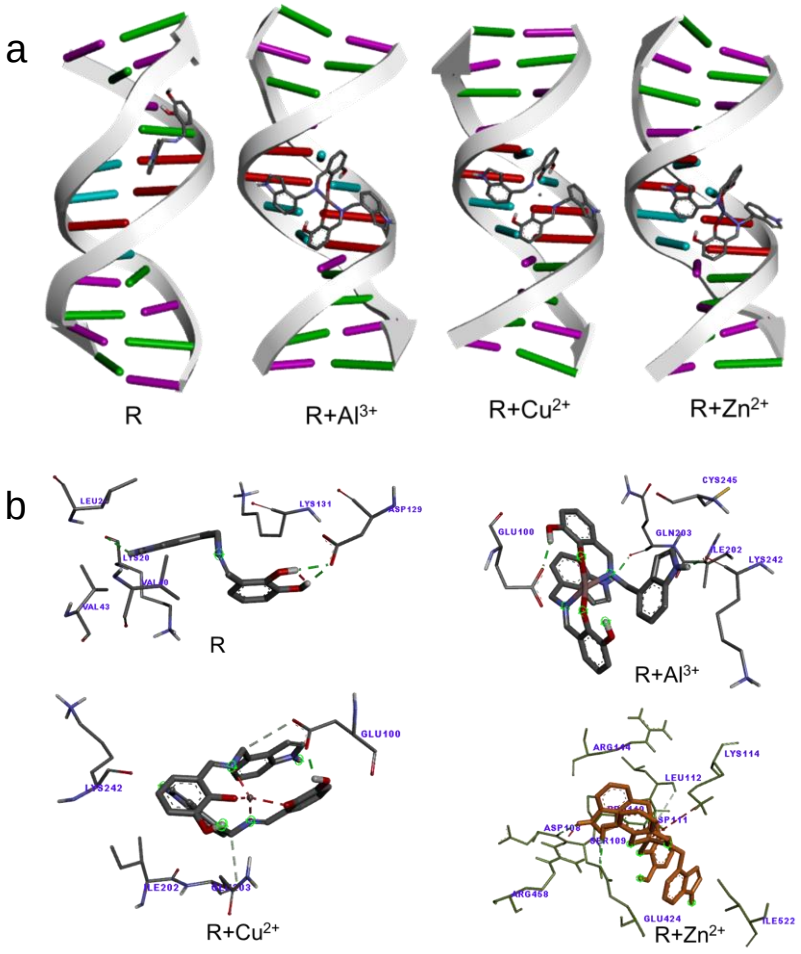

Fig. S20 (a) Molecular docking interaction of DNA with **R** and its metal complexes. (b) 3D diagram for the interaction mode of **R** and its metal complexes with BSA residues.

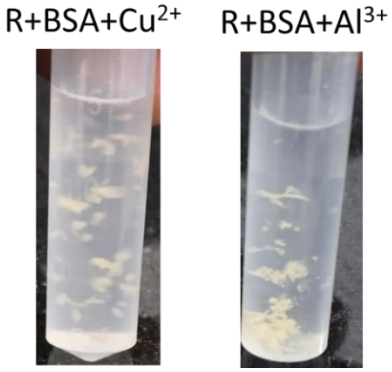

Fig. S21 Naked eye images of **R** (40 μM) + BSA (0.5 eq.) + M^{n+} (1 eq.) in in 7:3 CH_3CN/H_2O mixture at room temperature.

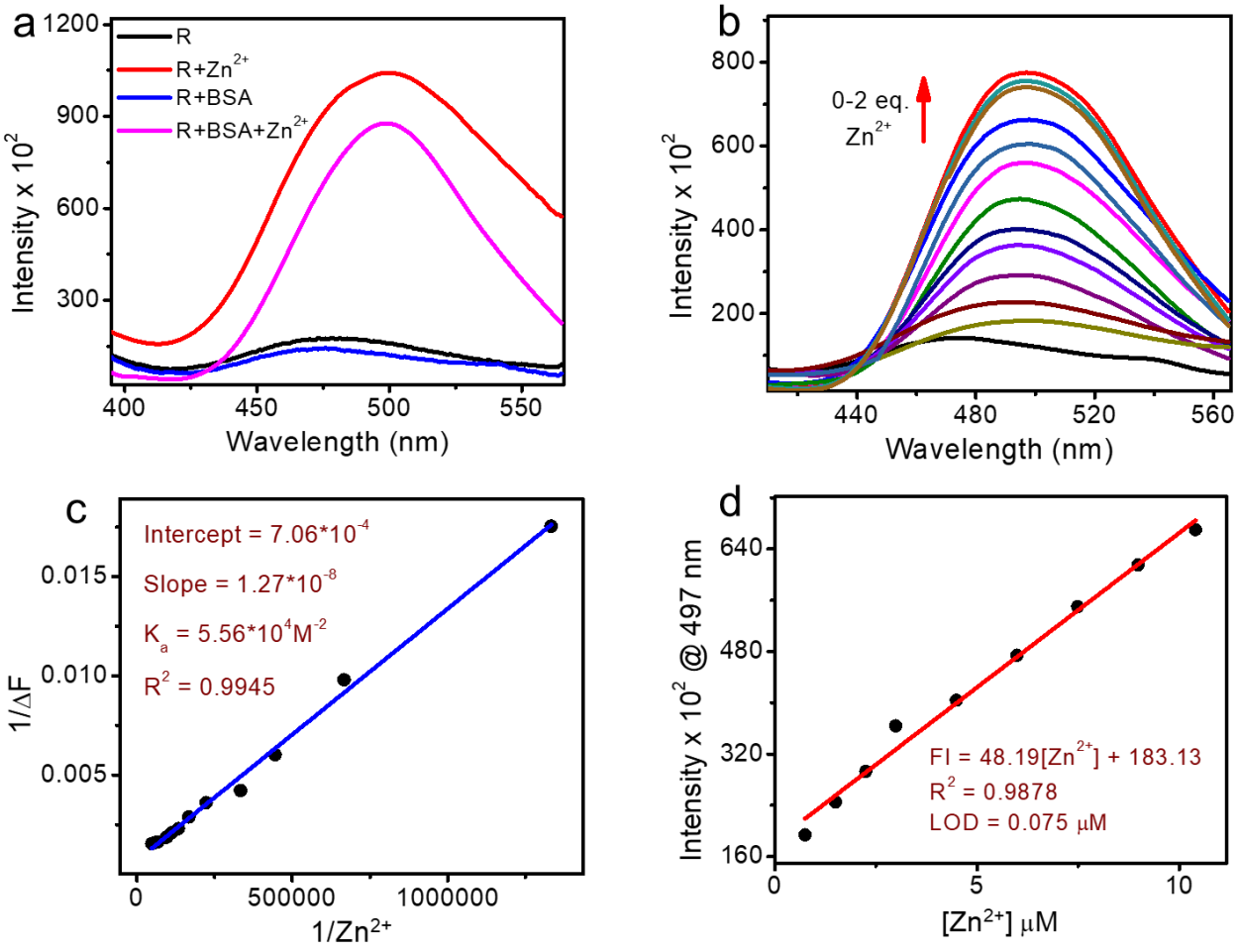

Fig. S22 (a) Fluorescence spectra of **R** (10 μM) with 1 eq. of BSA and 2 eq. of Zn^{2+} ions in CH3CN/H2O (7:3, v/v) medium at room temperature. (b) Variation in fluorescence spectra of **R** (10 μM) in the presence of Zn^{2+} ions (0-2 eq.) with BSA. (c) Benesi-Hildebrand plot of **R**-Zn^{2+} system with BSA. (d) Calibration curve of **R**-Zn^{2+} system with BSA.

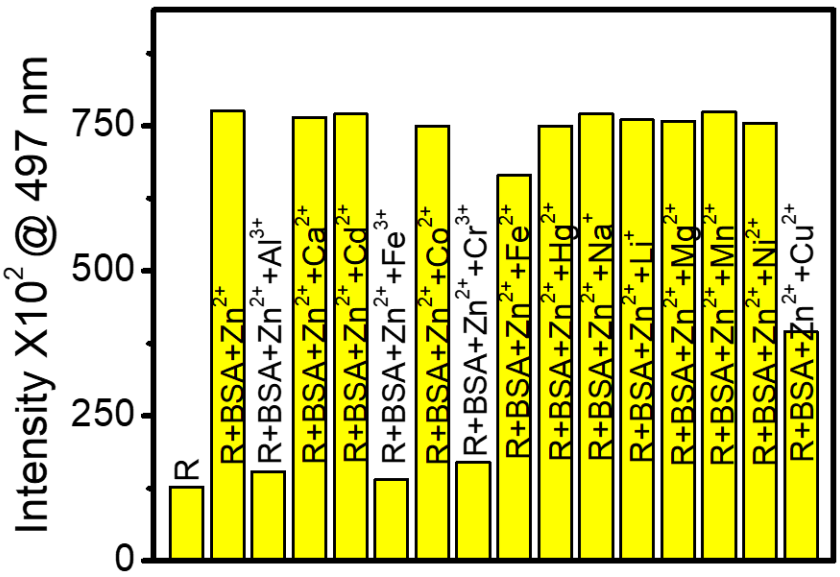

Fig. S23 Competitive study of **R**+Zn^{2+} complex over 2 eq. of various metal ions with BSA in CH_3CN/H_2O (7:3, v/v) medium at room temperature.

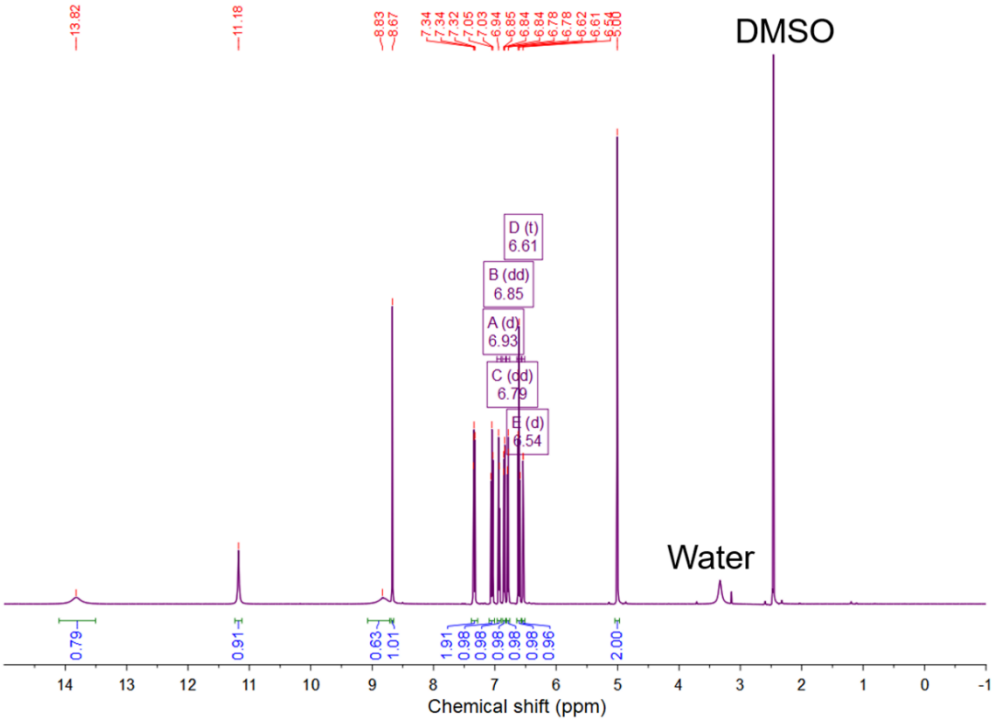

Fig. S24 ^{1}H NMR (500 MHz) spectrum of receptor **R** in d_6-DMSO at room temperature.

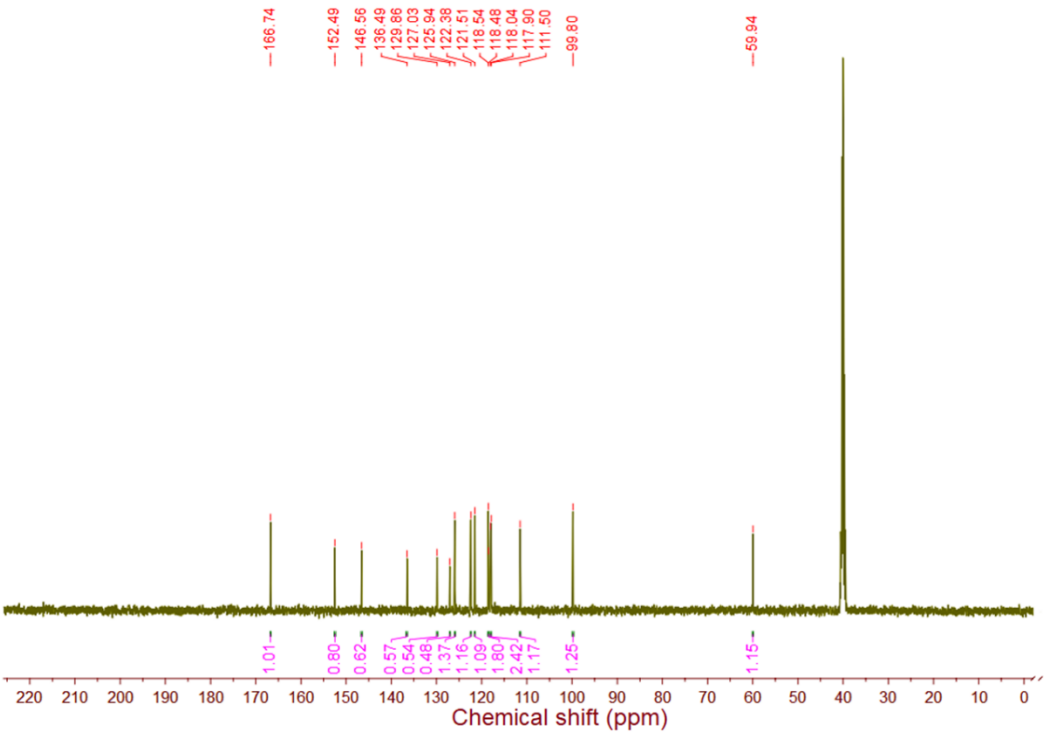

Fig. S25 ^{13}C NMR (125 MHz) spectrum of receptor **R** in d_6-DMSO at room temperature.

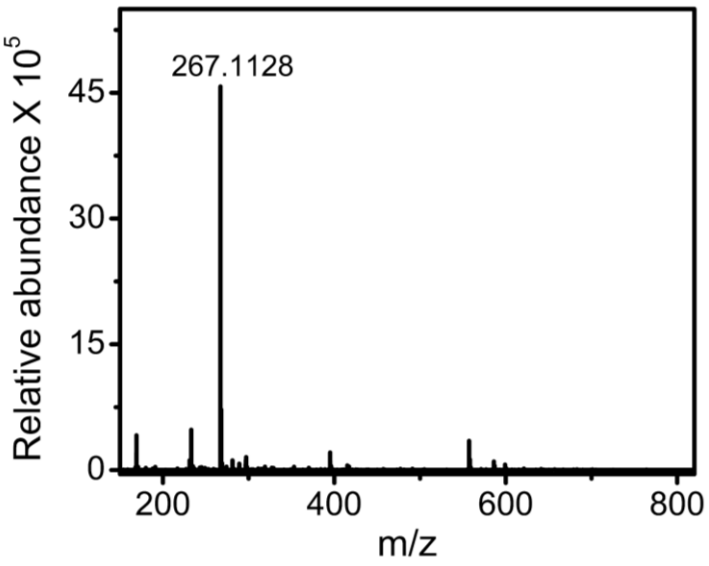

Fig. S26 ESI-MS spectrum of receptor **R**.

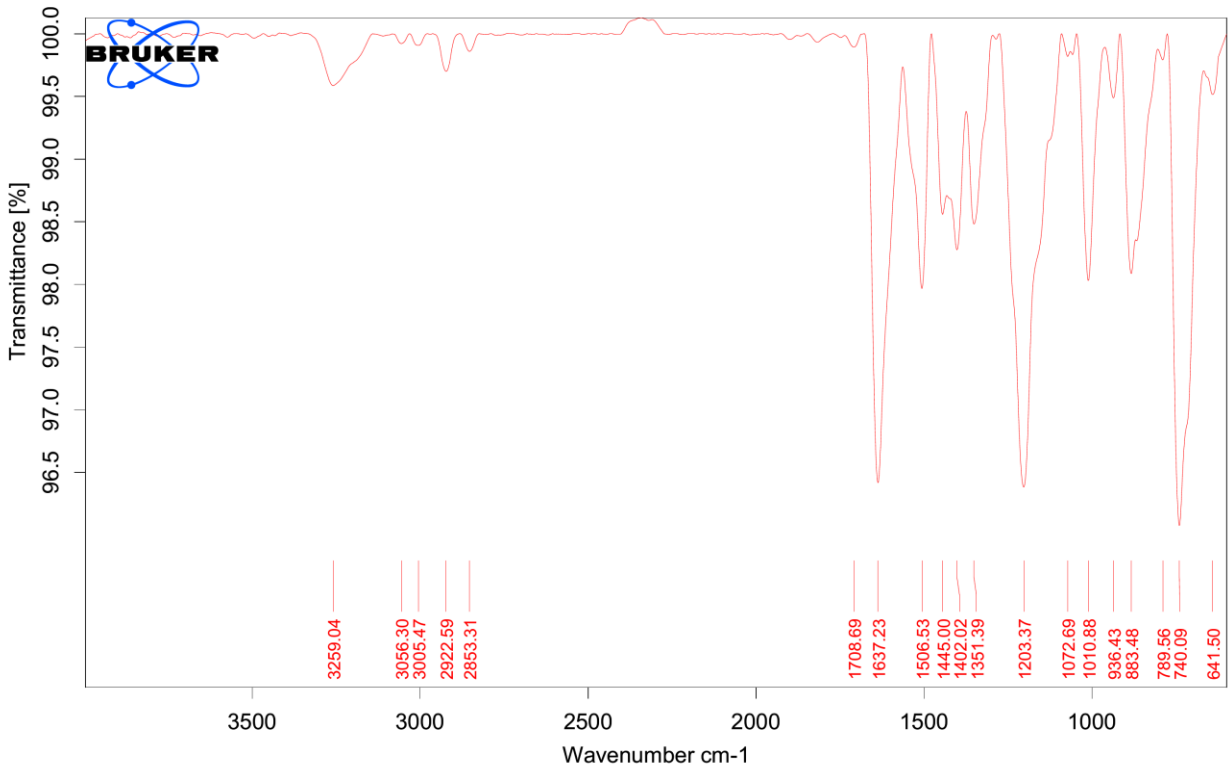

Fig. S27 Solid state IR spectrum of receptor **R**.

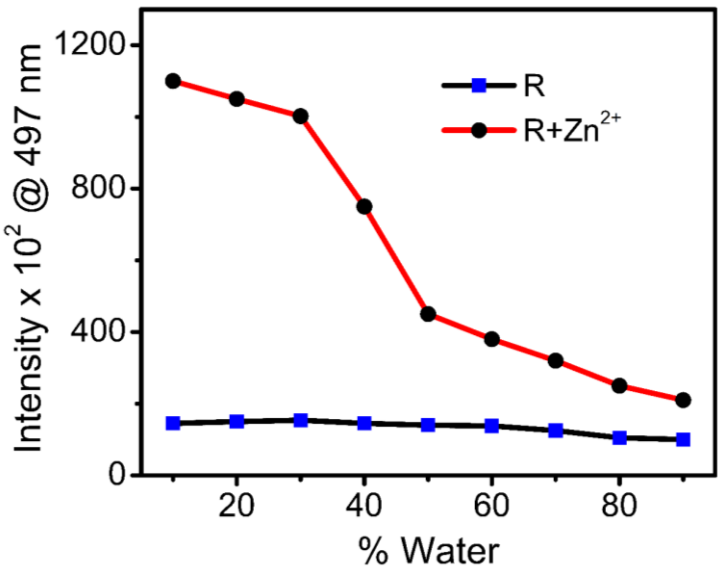

Fig. S28 Fluorescence spectral response of **R** and **R**+Zn^{2+} at different water fractions in CH_3CN.

Table S10. Determination of Cu^{2+} and Al^{3+} in tap and drinking water samples.

Samples	Cu^{2+} spiked (μM)	Al^{3+} spiked (μM)	Cu^{2+} found* (μM)	Al^{3+} found* (μM)	Recovery (%)	
					Cu^{2+}	Al^{3+}
Tap water	20	20	18.2 ± 0.20	19.15 ± 0.14	91.0	95.7
	40	40	37.1 ± 0.18	36.5 ± 0.2	92.7	91.3
Drinking water	20	20	18.9 ± 0.13	19.12 ± 0.27	94.5	95.6
	40	40	38.8 ± 0.16	38.2 ± 0.21	97.0	95.5

*Two replicates were performed

References

1 Y. L. Mu, C. J. Zhang, Z. L. Gao, X. Zhang, Q. Lu, J. S. Yao and S. Xing, *Synth. Met.,* 2020, **262**, 116334.

2 Y. W. Choi, J. J. Lee, E. Nam, M. H. Lim, and C. Kim, *Tetrahedron,* 2016, **72**, 1998–2005.

3 B. Jisha, M. R. Resmi, R. J. Maya and R. L. Varma, *Tetrahedron Lett.,* 2013, **54**, 4232–4236.

4 Z. Aydin and M. Keles, *Chem. Sel.,* 2020, **5**, 7375–7381.

5 M. Sahu, A. K. Manna, K. Rout, J. Mondal and G. K. Patra, *Inorg. Chim. Acta,* 2020, **508**, 119633.

6 A. K. Manna, J. Mondal, R. Chandra, K. Rout and G. K. Patra, *J. Photochem. Photobiol. A Chem.,* 2018, **356**, 477–488.

7 Heena, A. Silswal, D. Sharma, A. L. Koner, H. Om and R. Rana, *Spectrochim. Acta - Part A Mol. Biomol. Spectrosc.,* 2024, **320**, 124575.

8 S. M. Hossain, K. Singh, A. Lakma, R. N. Pradhan and A. K. Singh, *Sensors Actuators, B Chem.,* 2017, **239**, 1109–1117.

9 G. Ganesan, B. Pownthurai, N. K. Kotwal, M. Yadav, P. Chetti and A. Chaskar, *J. Photochem. Photobiol. A Chem.,* 2022, **425**, 113699.

10 Y. Zhang, Y. Fang, N. Z. Xu, M. Q. Zhang, G. Z. Wu and C. Yao, *Chinese Chem. Lett.,* 2016, **27**, 1673–1678.

11 (a) W. Li, Y. Zhang, X. Gan, M. Yang, B. Mie, M. Fang, Q. Zhang, J. Yu, J. Wu, Y. Tian and H. Zhou, *Sensors Actuators, B Chem.,* 2015, **206**, 640–646. (b) Y. Chang, B. Li, H. Mei, L. Yang, K. Xu, X. Pang, *Spectrochim. Acta Part A Mol. Biomol. Spectrosc.,* 2020, **226**, 117631.

12 D. Choe, H. So, S. Park, H. Lee, J. B. Chae, J. Kim, K. T. Kim, C. Kim, *Sensors,* 2021, **21**, 5591.